A Fractal Analysis of Surface Temperature Rise at Nano-Scale Sliding Contacts

Sudipto Roy[1] and S. K. Roy Chowdhury

Department of Mechanical Engineering,
Indian Institute of Technology, Kharagpur, India

ABSTRACT

A good deal of work has been carried out in recent years on temperature rise at the contact between sliding bodies with engineering scale roughness. However, as surfaces become smoother and loading decreases, in applications such as MEMS and NEMS devices, the analysis of surface temperature rise must consider the small-scale asperity height distributions and the surface forces those may be operating at small separations. The paper attempts to predict surface temperature rise at sliding contacts with small-scale roughness considering the influence of relevant parameters.

The results show in general that the contact surface temperature steadily increases with load, nano-scale roughness and surface forces. Interestingly, the fractal analysis presents a wide spectrum of solutions. While under certain combinations of fractal and material parameters extremely high contact temperature rise is predicted, under certain other parametric combinations extremely low temperature rise can be seen. The later parametric combination is certainly of much practical use.

Key Words: Surface temperature, nano-scale, surface roughness, surface forces and fractals.

1. Introduction

Surface temperature rise at the contact between sliding bodies is important since it influences friction and wear characteristics of the contacting bodies. Many attempts have been made to predict these temperatures analytically because measurement of the short-interval temperature rise at the asperity peaks is difficult. The work of Bloc [1], Jaeger [2], and Archard [3] set a pace for analytical work in this area. Ling [4], Gecim and Winer [5], Quinn and Winer [6] and many others have looked into the problem and proposed plausible solutions. The basic approach to the problem has been to consider that the frictional heat generated at the asperity tip is conducted away within a semi-infinite solid and to solve the one dimensional Fourier conduction equation with a constant heat flux at the surface of a semi-infinite body. Most of these and other earlier attempts considered only a single heat source but later it was realized that due to multi-asperity contacts the model must consider multiple heat sources. Guha and Roy Chowdhury [7] followed Archard's methodology but considered multiple heat sources to assess the effect of surface irregularities on the contact surface temperature under different load and speed conditions. In recent years, due to the wide spread development of magnetic storage devices, micro-electro-mechanical systems (MEMS) and nano-electro-mechanical systems (NEMS), there seems to be a need for predicting temperatures at the contact between surfaces with nano-scale roughness subjected to extremely low loads. In principle, assuming that the continuum is maintained, there is no difference in treating the heat conduction equation with multiple heat sources at the surfaces with macro, micro or nano scale roughness. However, with normal engineering surfaces, the effect of surface forces are negligible primarily because the separation between contacting surfaces is not small enough for the surface forces to be operative. The situation is different for nano-scale contacts and there surface molecular forces are likely to influence the contact geometry due to the small separations between the surfaces. A number of adhesion models have been developed to take into account the adhesive forces between ultra-smooth surfaces. These are valid at one end for rigid surfaces (Bradley theory) [8] to the other end for surfaces where large elastic deformation is caused by the adhesive forces (JKR theory) [9]. Surface roughness is an important factor in adhesion

[1] sudipto@mech.iitkgp.ernet.in

and effects of surface roughness on adhesion and contact area have been studied in great detail by Roy Chowdhury et al. [10] using Greenwood-Williamson [11] rough surface model. However, these multi-asperity models were for surfaces having roughness only on a narrow bandwidth of length scale and a Gaussian distribution of spherical asperities of uniform radius of curvature was found to closely represent such a surface [12]. It was later realized that those models were highly idealized; in fact real samples often exhibit a self-repeating nature, with morphological features superimposed on many different length scales [13]. In order to account for the effect of asperities ranging from nanometric to micrometric levels, it is therefore necessary to use a scale independent model. Fractal geometry, in detail fractal dimension, is thus necessary to quantitatively define self affinity [14]. Quite a few people [15, 16] have described the concept and development of fractal geometry and its application in characterizing rough surfaces and contact problems. The analysis of adhesion between rough solids using a fractal model has been studied in detail by Sahoo and Roy Chowdhury [17]. It was shown there that the fractal analysis gives a generalized solution and depending on the values of the fractal parameters, fractal dimension D and roughness G and material parameters, specific solutions can be obtained. The present paper presents a scale independent approach to predict surface temperature rise at the adhesive rough surface contacts between sliding bodies with nano-scale surface roughness.

2. Theoretical Background

Fractal geometry as an intrinsic parameter of surface topography has been widely used in recent years to characterize surface topography and contact mechanics. Majumdar and Tien [15], Majumdar and Bhushan [16] have used the fractal concept in contact mechanics problem quite elegantly. According to them, a representative contact configuration between an isotropic rough surface and a rigid flat plane results in contact spots of area 'a', which is related to the asperity deformation δ by $\delta = G^{D-1} a^{(2-D)/2}$. The contact spots produced during loading are spread randomly over the contact interface and may be of different sizes. The contact spot distribution n (a) is given as [18] $n(a) = \frac{D}{2} \frac{a_L^{D/2}}{a^{D/2+1}}$ where a_L is the area of the largest contact spot. The real area of contact over the surfaces, A_r is $A_r = \frac{D}{2-D} a_L$. A realistic approach to describe contacts between rough surfaces would be to consider that some of the contacting asperities are elastically and some plastically deformed [10]. In the fractal approach, the load on an elastically and plastically deformed asperity in the presence of surface forces is given by [17]

$$P_e = \frac{K G^{D-1} a^{(3-D)/2}}{\pi} - \frac{(6\gamma K)^{1/2} a^{3/4}}{\pi} \quad \text{and} \tag{1}$$

$$P_p = \frac{2Ha}{\pi} - \frac{2a^{D/2}\gamma}{\pi G^{D-1}} \quad \text{respectively.} \tag{2}$$

where γ is the surface energy per unit area, K the stiffness constant and H is the hardness of the softer material. The plasticity condition in terms of non-dimensional fractal parameters

$G^* (G = G/A_a^{1/2})$ and a^* $(a = a/A_a)$, is given as [17]

$$\left(a^*\right)^{(3/4-D/2)} - \frac{\lambda^*}{\theta^*}\left(a^*\right)^{1/4} - \left(\frac{6}{\theta^*}\right)^{1/2} \geq 0 \tag{3}$$

where θ^*, termed as fractal elastic adhesion index, is the ratio of the elastic force to the adhesive force experienced by an asperity and is defined as [22] $\theta^* = \frac{K\sqrt{A_a}}{\gamma}\left(G^*\right)^{2(D-1)}$ while fractal plastic adhesion

index λ^* is the ratio of the force required for plastic yielding to the adhesive force on an asperity and is given as $\lambda^* = \frac{H\sqrt{A_a}}{\gamma}\left(G^*\right)^{(D-1)}$. Solution to equation (3) gives the non-dimensional apparent critical contact spot area a_{c1}^* which can be related to the non-dimensional real contact spot area a_c^* as

$$\left(a_c^*\right)^{(1-D/2)} = \left(a_{c1}^*\right)^{(1-D/2)} - \frac{2\sqrt{6}}{3}\left(\theta^*\right)^{(-1/2)}\left(a_{c1}^*\right)^{1/4} \tag{4}$$

Thus, contacts spots of area $a^* > a_c^*$ are plastically deformed. The total applied load on a rough surface can then be obtained by summing up the load contributions on all the elastically and plastically deformed asperities and may be given in non-dimensional form as

$$P_a^* = \frac{D}{\pi}\left(a_L^*\right)^{D/2}\left[\frac{1}{2}\int_{a_{s1}^*}^{a_{c1}^*}\left\{\left(a^*\right)^{(1-2D)/2} - \left(\frac{6}{\theta^*}\right)^{1/2}\left(a^*\right)^{(-1-2D)/4}\right\}\,da^* + \int_{a_c^*}^{a_L^*}\left\{\left(\frac{\lambda^*}{\theta^*}\right)\left(a^*\right)^{(-D/2)} - \frac{1}{\theta^*}\left(\frac{1}{a^*}\right)\right\}\,da^*\right] \tag{5}$$

where $P_a^* = \frac{P_a}{KA_a\left(G^*\right)^{D-1}}$, a_L^* is the dimensionless largest contact spot area and a_{s1}^* is the dimensionless apparent smallest contact spot area corresponding to the smallest spot area a_s, which tends to zero.

3. Contact surface temperature: General methodology

In most flash temperature analyses the total heat generation is assumed to be due to the frictional loss at the contact surface although some heat generation may occur within the plastically deforming near surfaces of the contacting bodies. Following the work of Blok [1] and Jaeger [2], flash temperature has been analytically evaluated hitherto on the assumption that the frictional heat is generated at the real area of contact and the heat is mainly conducted away into the bulk of the rubbing surface although in some cases convective and radiation loses have also been considered [6,7]. There are three important issues in carrying out such an analysis. Firstly, the division of heat into the rubbing bodies needs to be quantified. In this regard, Blok [1] defined a heat partition factor ζ which can be obtained by equating the maximum temperatures of the two surfaces at the contact and is given as $\zeta = \frac{k_1}{k_1 + k_2}$ Secondly a speed parameter $L \equiv \frac{vr\rho C}{2k}$ is used to distinguish between slow and fast moving contacts [4]. Here, v is the sliding speed, r the contact radius, ρ the density, C the specific heat and k the thermal conductivity of the material. In general, for stationary or slow moving heat sources L is less than 0.1 and for fast moving heat sources, L is greater than 5. For stationary or slow moving heat sources, the heat flow Q is usually obtained from an electrical analogy and the average temperature for such contacts is given by [18]

$$\Theta_{ls} = \frac{Q}{4k}\left(\frac{\pi}{a}\right)^{1/2} \tag{6}$$

Under these conditions there is sufficient time for the temperature distribution of a stationary contact to be established. However for fast moving heat sources equation (6) is not applicable. For fast moving contacts the problem can be treated as a transient heat flow in a semi-infinite solid with a constant heat flux at the surface. The average surface temperature may then be written as [2]

$$\Theta_{hs} = \frac{4\sqrt{2}}{3}\frac{Q}{(a\pi)^{3/4}\left(k\rho Cv\right)^{1/2}} \tag{7}$$

Thirdly, the mode of asperity deformation also need be identified since this would affect the heat generation at the contact spots. In the present model we consider that the asperities on the contacting surfaces may either be elastically or plastically deformed and the plasticity criterion of equation (3) would be used to differentiate between the two cases. In addition among all the elastically or plastically deformed contact spots some would fall in the low speed and some in the high speed regimes. In finding the average contact temperature between two rubbing solids, temperature at the peaks of all the four different categories of contact spots are determined and averaged. This is attempted in the following section.

3.1 Fractal modeling of flash temperature

The heat flow rate for an elastically and plastically deformed contact spot are given by $Q=\zeta\mu P_e v$ and $Q=\zeta\mu P_p v$ respectively. Then, substituting equation (1) and (2) in equation (6) the average temperature rise for an elastically and plastically deformed contact spot in the slow speed regime can be given in terms of fractal parameters as:

$$\Theta_{avlse} = \frac{\zeta\mu v}{4k_1\sqrt{\pi}}\left[KG^{(D-1)}a^{(2-D)/2} - (6\gamma K)^{1/2}a^{1/4}\right] \tag{8}$$

$$\Theta_{avlsp} = \frac{\zeta\mu v}{2k_1\sqrt{\pi}}\left[H\sqrt{a} - \frac{a^{(D-1)/2}\gamma}{G^{(D-1)}}\right] \tag{9}$$

where the subscripts avlse and avlsp, refer to "average, low speed, elastic"and "average, low speed, plastic" respectively. The average flash temperature rise for an elastically and plastically deformed single contact spot in the high speed regime can similarly be obtained by substituting equation (1) and (2) in equation (7) and may be given as:

$$\Theta_{avhse} = \frac{0.80\zeta\mu v^{1/2}}{(k_1\rho_1 C_1)^{1/2}}\left[KG^{(D-1)}a^{(3-2D)/4} - (6\gamma K)^{1/2}\right] \tag{10}$$

$$\Theta_{avhsp} = \frac{0.80\zeta\mu v^{1/2}}{(k_1\rho_1 C_1)}\left[Ha^{1/4} - \frac{a^{(2D-3)/4}\gamma_1}{G^{(D-1)}}\right] \tag{11}$$

where the subscripts avhse and avhsp refer to "average, high speed, elastic" and "average, high speed, plastic" respectively.

3.2 Average flash temperature over the contact zone

The total flash temperatures at all the contact spots belonging to each group can now be obtained in non-dimensional form as

$$\Theta^*_{tlse} = \int_{a^*_{sl}}^{a^*_{ls}} \frac{\mu}{4Fo^{1/2}}\left[\left(a^*\right)^{\frac{2-D}{2}} - \left(\frac{6}{\theta^*}\right)^{1/2}\left(a^*\right)^{1/4}\right] n(a^*)\,d(a^*) \tag{12}$$

$$\Theta^*_{tlsp} = \int_{a^*_c}^{a^*_{lsp}} \frac{\mu}{2\sqrt{2Fo}}\left[\left(\frac{\lambda^*}{\theta^*}\right)\left(a^*\right)^{1/2} - \frac{1}{\theta^*}\left(a^*\right)^{(D-1)/2}\right] n(a^*)\,d(a^*) \tag{13}$$

$$\Theta^*_{thse} = \int_{a^*_{hs}}^{a^*_{sl}} \frac{2\sqrt{2}\mu}{\pi}\left[\left(a^*\right)^{(3-2D)/4} - \left(\frac{6}{\theta^*}\right)^{1/2}\right] n(a^*)\,d(a^*) \tag{14}$$

$$\Theta^*_{thsp} = \int_{a^*_{hsp}}^{a^*_L} \frac{2^{7/4}\mu}{\pi}\left[\left(\frac{\lambda^*}{\theta^*}\right)\left(a^*\right)^{1/4} - \frac{1}{\theta^*}\left(a^*\right)^{(2D-3)/4}\right] n(a^*)\,d(a^*) \tag{15}$$

where the subscripts tlse, tlsp, thse and thsp refer to "total, low speed, elastic", "total, low speed, plastic", "total, high speed, elastic" and "total, high speed, plastic" respectively and a_{lse}^*, a_{lsp}^*, a_{hse}^*, a_{hsp}^* represent contact spot area under low speed-elastically deformed, low speed-plastically deformed, high speed-elastically deformed and high speed-plastically deformed conditions respectively. The Fourier number Fo here is a measure of heat conducted through a body relative to the heat stored and a large value of Fo would indicate a faster propagation of heat through the body.

Therefore, the cumulative non-dimensional contact temperature rise, Θ^*_{total} over the entire contact zone is the sum of the temperatures in equations (12)-(15) and the average flash temperature over the entire contact zone in non-dimensional form would be

$$\Theta^*_{av} = \frac{1}{n'}\left(\Theta^*_{total}\right) \tag{16}$$

where n' the total number of contact spots between $a_{sl} < a < a_L$ is given by $n' = \int_{a_{sl}^*}^{a_L^*} n(a^*)d\left(a^*\right)$

Evaluating equation (16) along with equations (12)-(15) we may find the average flash temperature over the entire contact zone with different parametric variations. It can be seen that there are atleast four important parameters, viz. D, θ^*, λ^* and applied load, that decide the trend of flash temperature. The physical significance of fractal dimension is that as D increases the high frequency components become comparable to the low frequency ones and it has been shown that adhesion is significantly influenced by D possibly because of the contribution made by the high frequency signals [13, 17]. Fractal adhesion indices θ^*, and , λ^* as explained earlier indicate the relative importance of adhesion and surface roughness. Since temperature at the contact between surfaces with nano-scale roughness is likely to be influenced by adhesion it is important to consider first the influence of these parameters on adhesion. Unloading or separation between rough solids has been analyzed using a fractal approach elsewhere [17] and following this 3-D plots of adhesion force against θ^*, and , λ^* for two extreme values of D, 1.1 and 1.9 at a particular applied non-dimensional load are shown in figures- 1(a) and (b). It can be seen in figure-1 that adhesion reaches a peak value at θ^*, ranging between 1 and 10^3 depending on the parametric combination of non-dimensional applied load, λ^* and D. It can also be seen in figures-1(a) and (b) that the adhesion force decreases with increasing, λ^* and becomes insignificant at values of , λ^* around 10^4 for a wide combination of θ^*, and D.

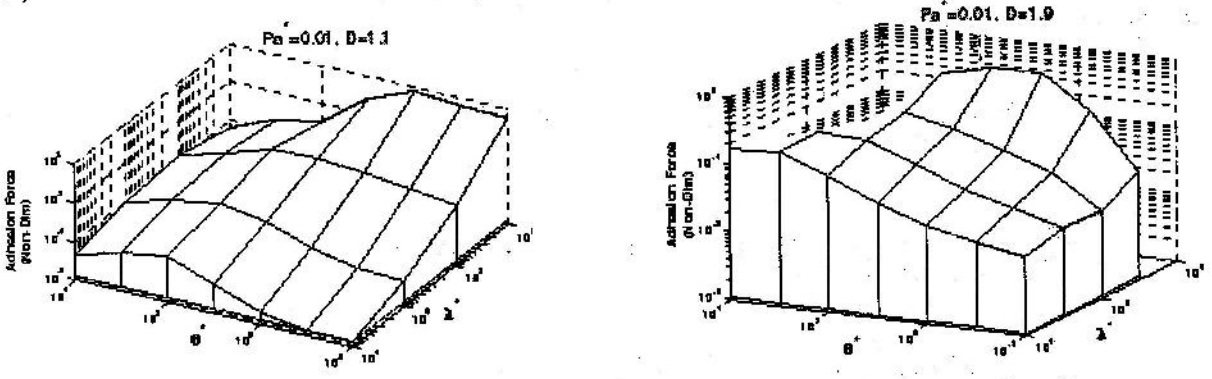

Figure-1 Plot of non-dimensional adhesion force against adhesion indices for (a) D=1.1 (b) D=1.9.

In order to show the effect of variation of θ^* on flash temperature it is necessary to chose a value of λ^* that has a negligible effect on adhesion. Average flash temperature has been plotted in figure-2(a) against θ^* for $\lambda^* = 10^4$ and for different values of dimension D at a given non-dimensional applied load, Pa*=0.01. It is seen that flash temperature is high within the range of θ^* for which force of adhesion is significant

and it decreases as this range of θ^* is exceeded. To show the effect of variation of λ^* on flash temperature, θ^* was chosen as 1 and figure-2(b) was plotted for different values of D. It is seen that average flash temperature is high at low values of λ^* and decreases with increasing λ^* and becomes very low for λ^* values around 10^4. The range of θ^* and λ^* for which flash temperature is high also depends on the value of D, as is evident from figure-2 and 3 respectively and this matches with the trend of adhesion plots with D in figure-1. It is also interesting to note that with D the flash temperature initially decreases till around D=1.5 and then rises with an increase in D for some combination of θ^* and λ^*. However the value of D at which the reversal occurs depends on the combination of θ^* and λ^*. This reversal in behavior with varying D has been observed by Majumdar and Bhushan [13] in their fractal model for real area of contact and also by Sahoo and Roy Chowdhury [17] in their fractal model for adhesional friction between rough surfaces. Plots of non-dimensional average flash temperature against non-dimensional applied load for different combinations of θ^* and λ^* in the significant adhesion zone and two extreme values of dimension D (1.1 and 1.9), are shown in figure-3. It is seen that the temperature increases monotonically with the applied load but the temperature levels are significantly influenced by the fractal dimension D.

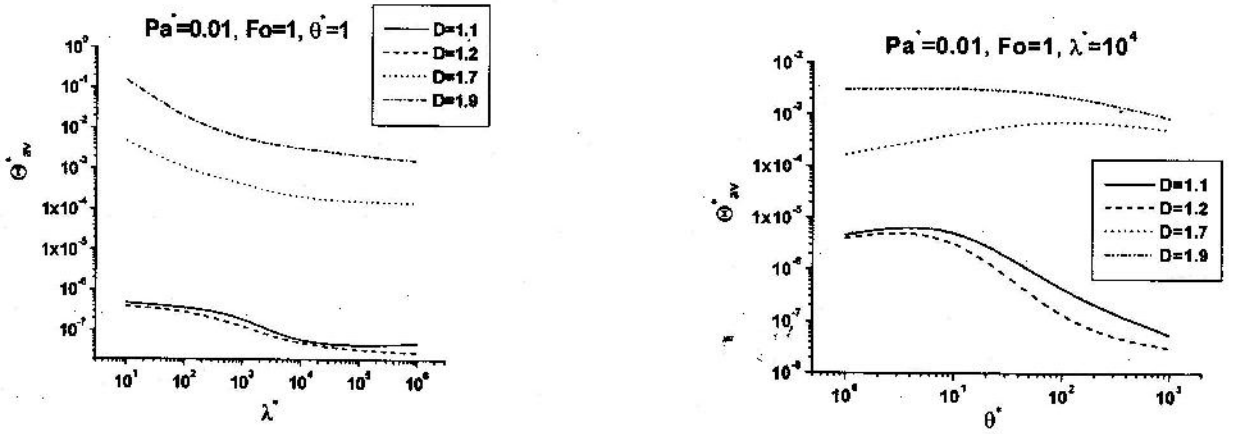

Figure-2 Plots of non-dimensional average flash temperature against (a) θ^* (b) λ^*

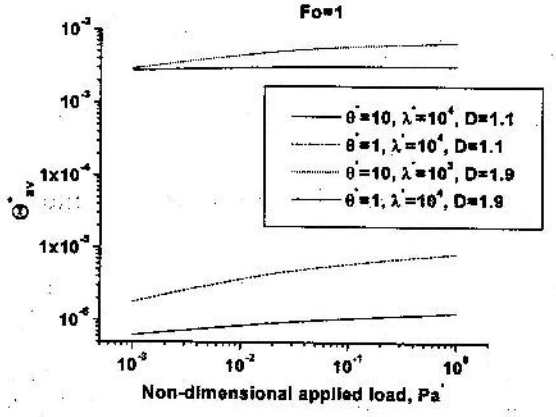

Figure-3: Plot of non-dimensional average flash temperature against non-dim. applied normal load.

Conclusion

The paper attempts to present a fractal analysis of contact temperature rise between sliding bodies with nano-scale surface roughness. A surface here is considered to comprise four distinct types of contact spots namely, low speed elastic, low speed plastic, high speed elastic and high speed plastic. The presence of surface forces at the contact was taken into account in the contact mechanics analysis and the contact temperature rise at all the contact spots have been averaged. The effects of surface and material properties

have been demonstrated. Large adhesion at the interface may yield very high contact temperature rise whereas some other combinations of material and surface parameters may yield almost insignificant rise in contact temperature.

References

[1] Block, H., General discussion on lubrication , Proc. Inst. Mech. Eng., 1937,2, 222-235.

[2] Jaeger, J.C., Moving sources of heat and the temperature at sliding surfaces, Proc. R. Soc. N.S.W., 1942, 66, 203-224.

[3] Archard, J.F., The temperature of rubbing surfaces, Wear, 1959, 2, 438-455.

[4] Ling, F. F., On temperature transients in sliding interface, Trans. ASME, J. Lubr. Technol., 1969, 91, 397-405.

[5] Gecim,B. & Winer, W.O., Transient temperatures in the vicinity of an asperity contact,ASME J. Tribol., 1985, 107, 333-342.

[6] Quinn, T.F.J. & Winer, W.O., The thermal aspects of oxidational wear, Wear, 1985, 102, 67- 80.

[7] Guha, D. and Roy Chowdhury S.K., The effect of surface roughness on the temperature at the contact between sliding bodies, Wear, 1996, 197 63-73.

[8] Bradley, R. S., The cohesive force between solid surfaces and the surface energy of solids, Phil. Mag.1932, 13, 853-862.

[9] Johnson, K.L., Kendall, K., Roberts, A.D., Surface energy and the contact of elastic solids, Proc. R.Soc. London 1971, A 324, 301-313.

[10] Roy Chowdhury, S.K. and Ghosh, P., Adhesion and adhesional friction at the contact between solids., Wear, 1994, 9-19.

[11] Greenwood, J.A. and Williamson, J.B.P., Contact of nominally flat surfaces, Proc. R. Soc.London, 1966, A295, 300-319.

[12] Sayles, R.S. and Thomas, T.R., Surface topography as a non-stationary random process, Nature, 1978, 271, 431-434.

[13] Majumdar, A. and Bhushan, B., Fractal model of elastic-plastic contact between rough surfaces, J.Tribol.-Trans. ASME 1991, 113, 1-11.

[14] Mandelbrot, B.B., How long is the coastline of Britain? Statistical self-similarity and fractional dimension, Science, 1967, 155, 636-638.

[15] Majumdar, A. and Tien, C.L., Fractal characterization and simulation of rough surfaces, Wear, 1990, 136, 313-327.

[16] Majumdar, A. and Bhushan, B., Role of fractal geometry in roughness characterization and contact mechanics of surfaces, J. Tribol.-Trans. ASME, 1990, 112, 205-216.

[17] Sahoo, P. and Roy Chowdhury, S.K., A fractal analysis of adhesion at the contact between rough solids., J. Engg. Tribology: Proc. Instn. Mech.Engrs, 1996, 210,269-279.

[18] Holm, R., Calculation of the temperature development in a contact heated in the contact surface and application to the problem of the temperature rise in a sliding contact, J. Appl. Phys., 1948, 19, 361-366.

——— • • • ———